Science Advances
AAAS

Supplementary Materials for

Gas-phase detection of oxirene

Jia Wang *et al.*

Corresponding author: Alexander M. Mebel, mebela@fiu.edu; André K. Eckhardt, andre.eckhardt@rub.de; Ralf I. Kaiser, ralfk@hawaii.edu

Sci. Adv. **9**, eadg1134 (2023)
DOI: 10.1126/sciadv.adg1134

This PDF file includes:

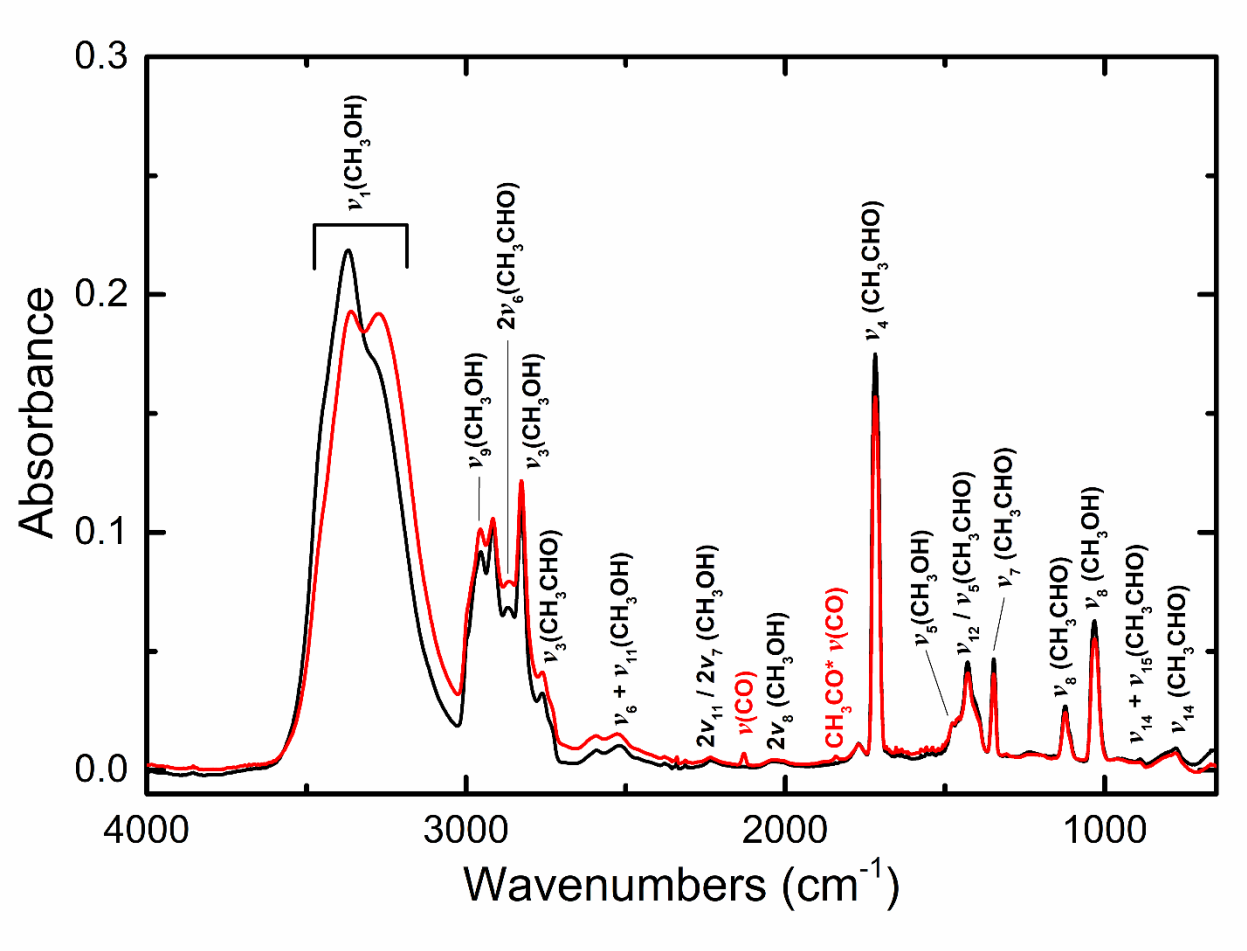

Fig. S1.
FTIR spectra of CH_3OH–CH_3CHO ices at 5 K before (black line) and after (red line) irradiation at 20 nA for 15 minutes. Detailed assignments are listed in table S1.

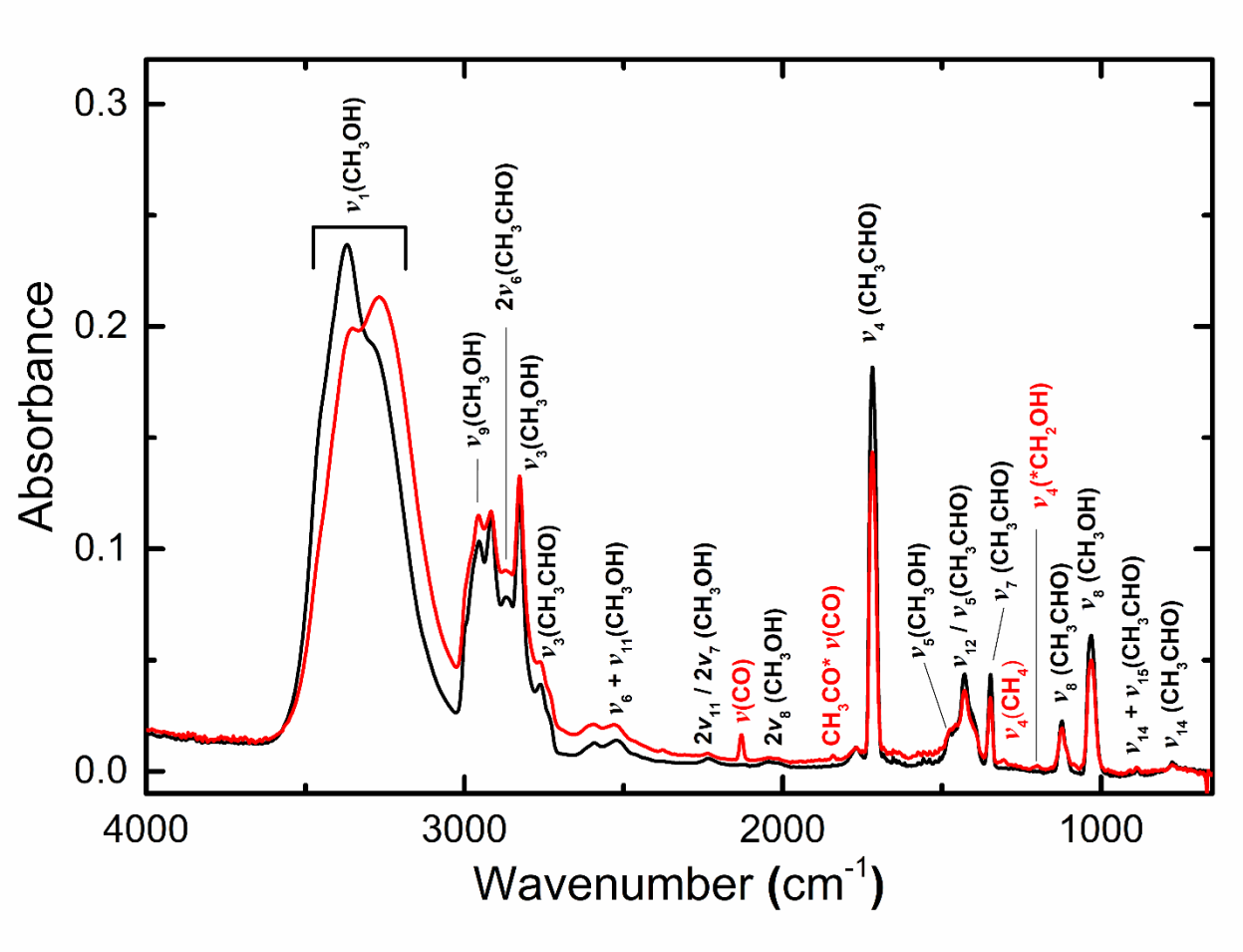

Fig. S2.
FTIR spectra of CH_3OH–CH_3CHO ice at 5 K before (black line) and after (red line) irradiation at 20 nA for 60 minutes. Detailed assignments are listed in table S2.

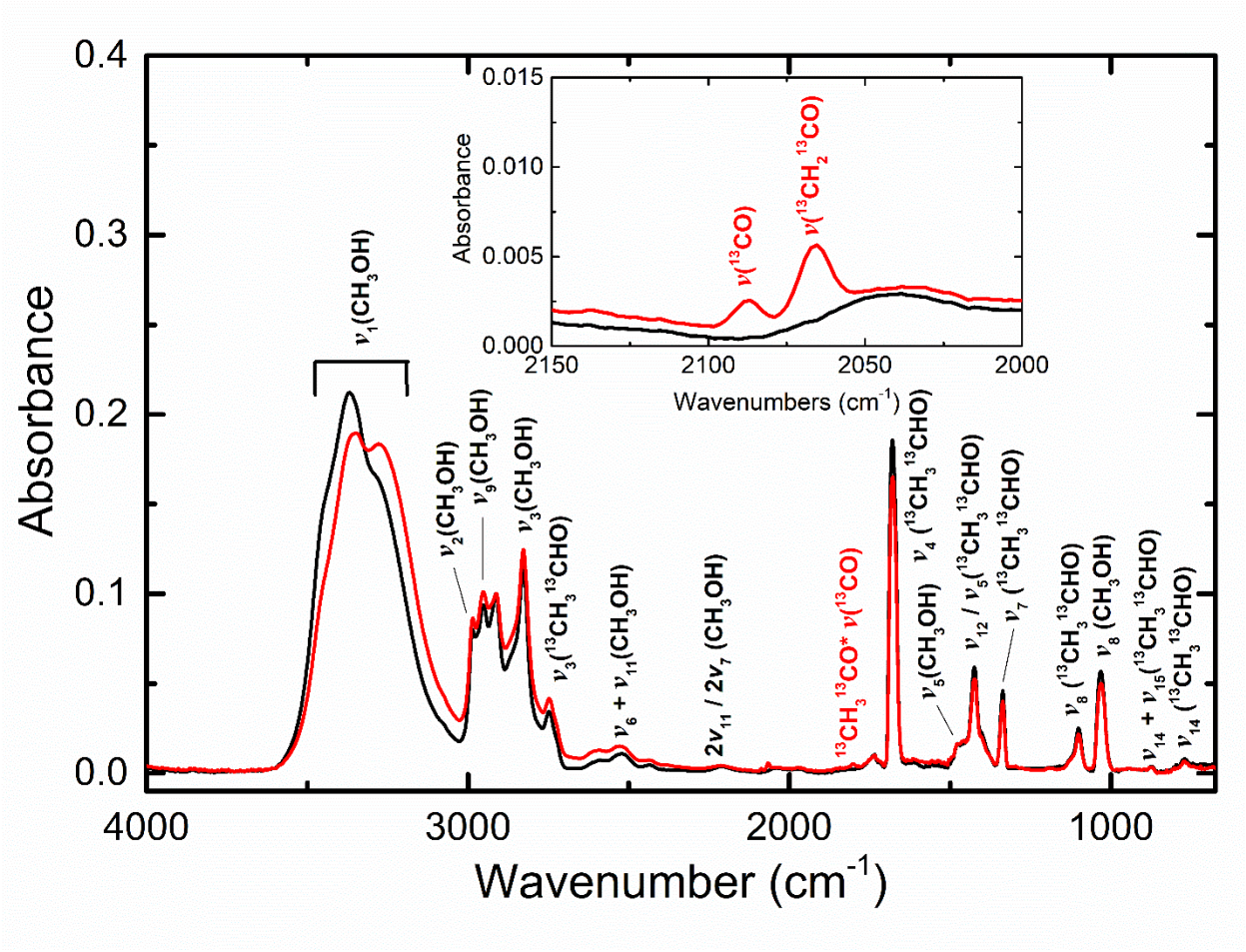

Fig. S3.
FTIR spectra of CH_3OH–$^{13}CH_3{}^{13}CHO$ ices at 5 K before (black line) and after (red line) irradiation at 20 nA for 15 minutes. Detailed assignments are listed in table S3. Inset: Zoom in between 2150 and 2000 cm^{-1} showing new peaks after irradiation corresponding to ^{13}CO and ketene-$^{13}C_2$.

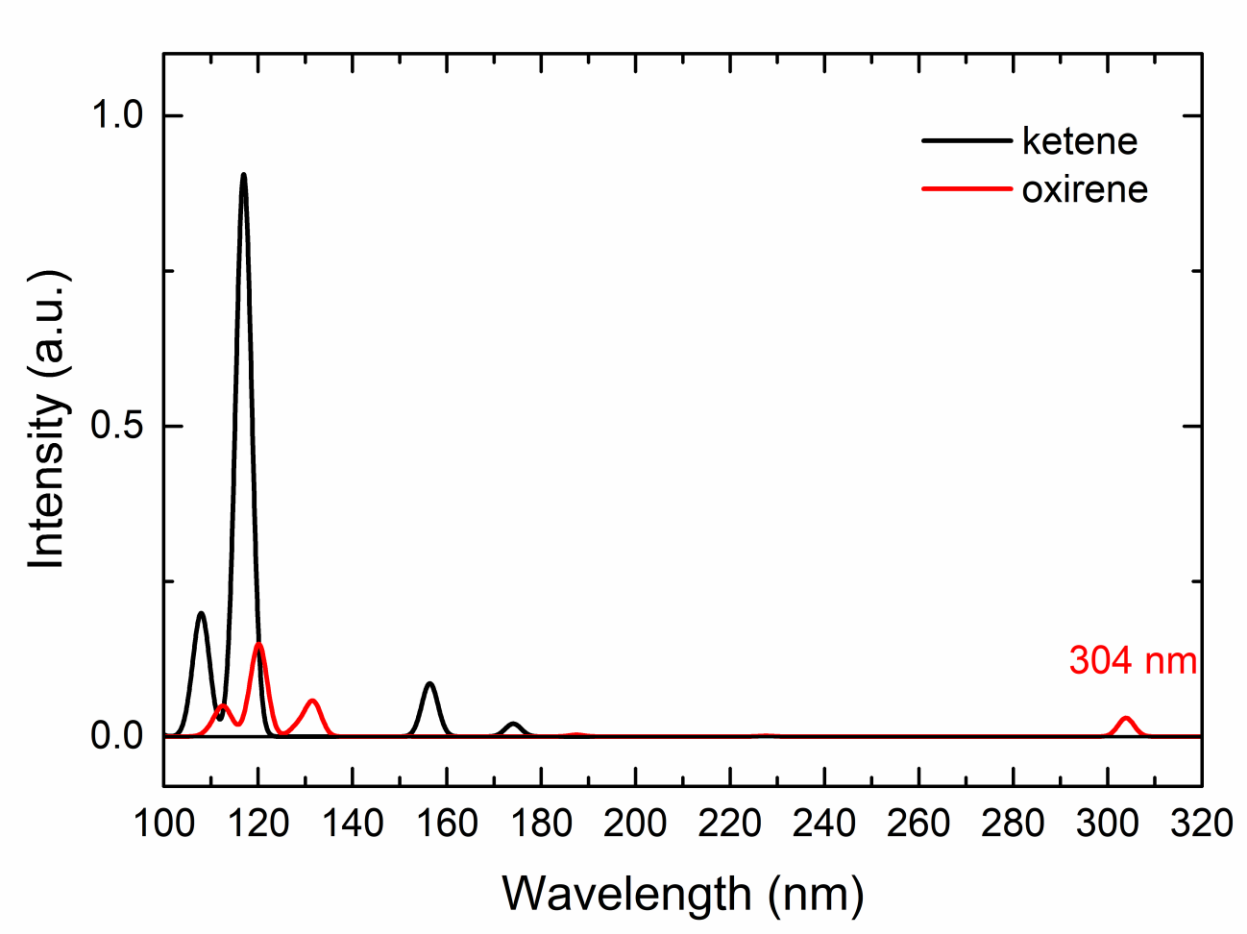

Fig. S4.
Simulated ultraviolet-visible (UV-Vis) spectra of ketene and oxirene calculated at the TD-PBE0/cc-pVTZ level of theory. The spectra were convoluted using a Gaussian line shape function with a full width at half maximum (FWHM) of 4 nm.

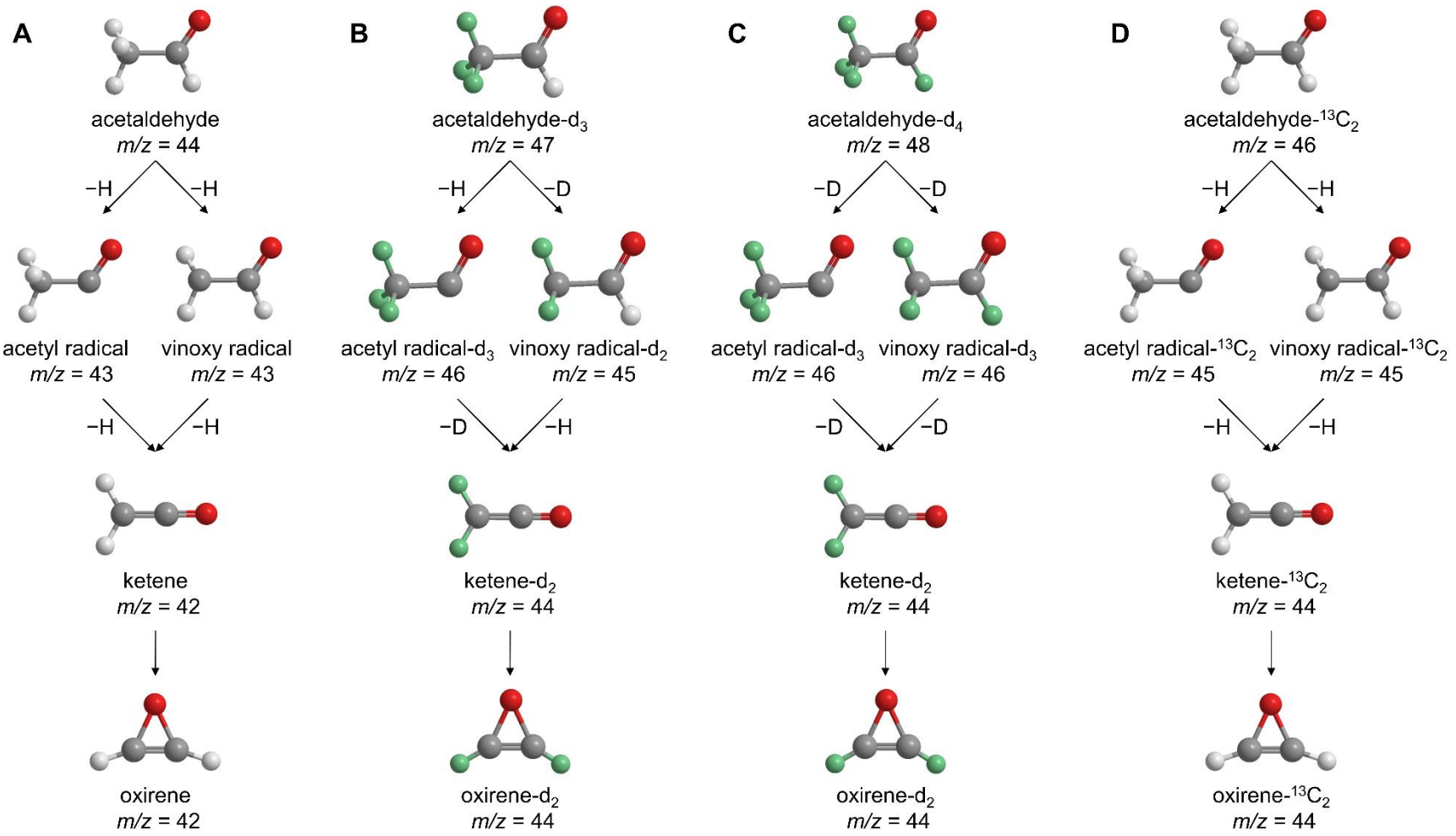

Fig. S5.
Formation schemes of ketene and oxirene. Reaction schemes showing pathways from acetaldehyde (**A**), acetaldehyde-d_3 (**B**), acetaldehyde-d_4 (**C**), and acetaldehyde-$^{13}C_2$ (**D**) to ketene and oxirene. The atoms are color-coded in white (hydrogen), light blue (deuterium), gray (carbon), and red (oxygen).

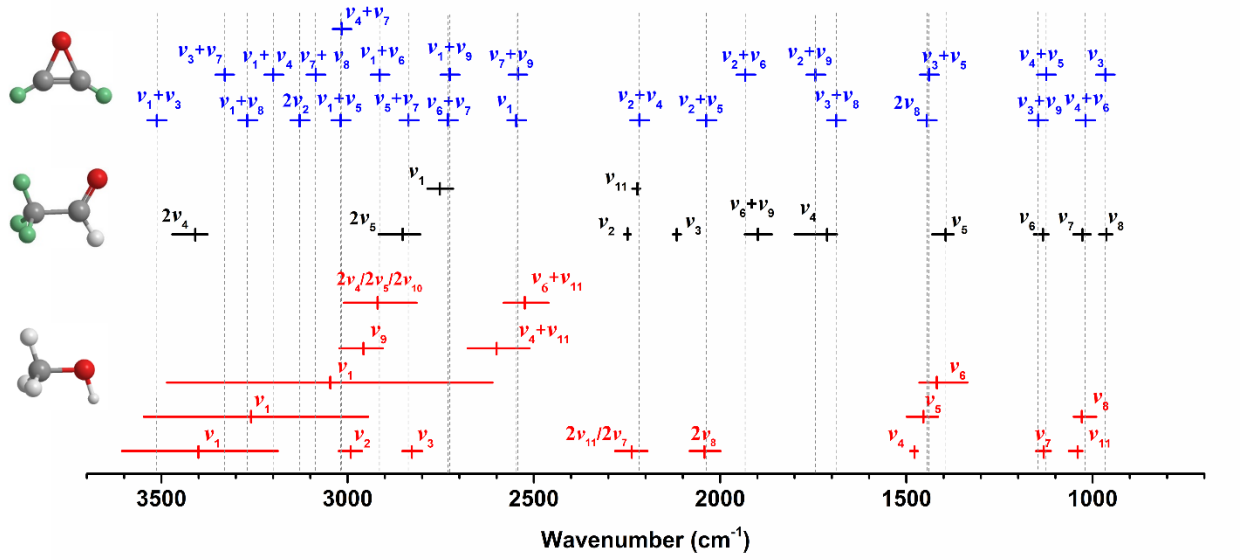

Fig. S6. Peak absorptions (solid vertical lines) and absorption ranges (solid horizontal lines) of methanol (CH_3OH, red), acetaldehyde-d_3 (CD_3CHO, black), and oxirene-d_2 (*c*-C_2D_2O, blue). Dotted vertical lines indicate the overlap positions between the absorption peaks of oxirene-d_2 and reactants (CH_3OH, red; CD_3CHO, black). Detailed absorption positions and assignments for experimentally measured pure methanol and acetaldehyde-d_3 ices as well as calculated oxirene-d_2 are listed in table S6.

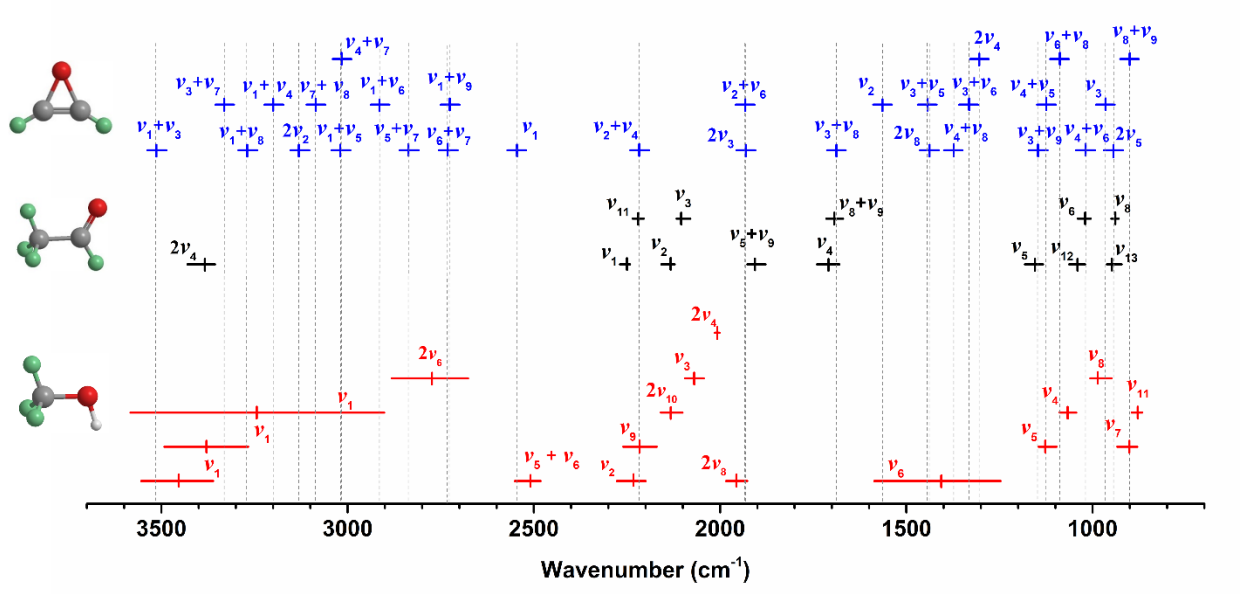

Fig. S7. Peak absorptions (solid vertical lines) and absorption ranges (solid horizontal lines) of methanol-d$_3$ (CD_3OH, red), acetaldehyde-d$_4$ (CD_3CDO, black), and oxirene-d$_2$ (*c*-C_2D_2O, blue). Dotted vertical lines indicate the overlap positions between the absorption peaks of oxirene-d$_2$ and reactants (CD_3OH, red; CD_3CDO, black). Detailed absorption positions and assignments for experimentally measured pure methanol-d$_3$ and acetaldehyde-d$_4$ ices as well as calculated oxirene-d$_2$ are listed in table S7.

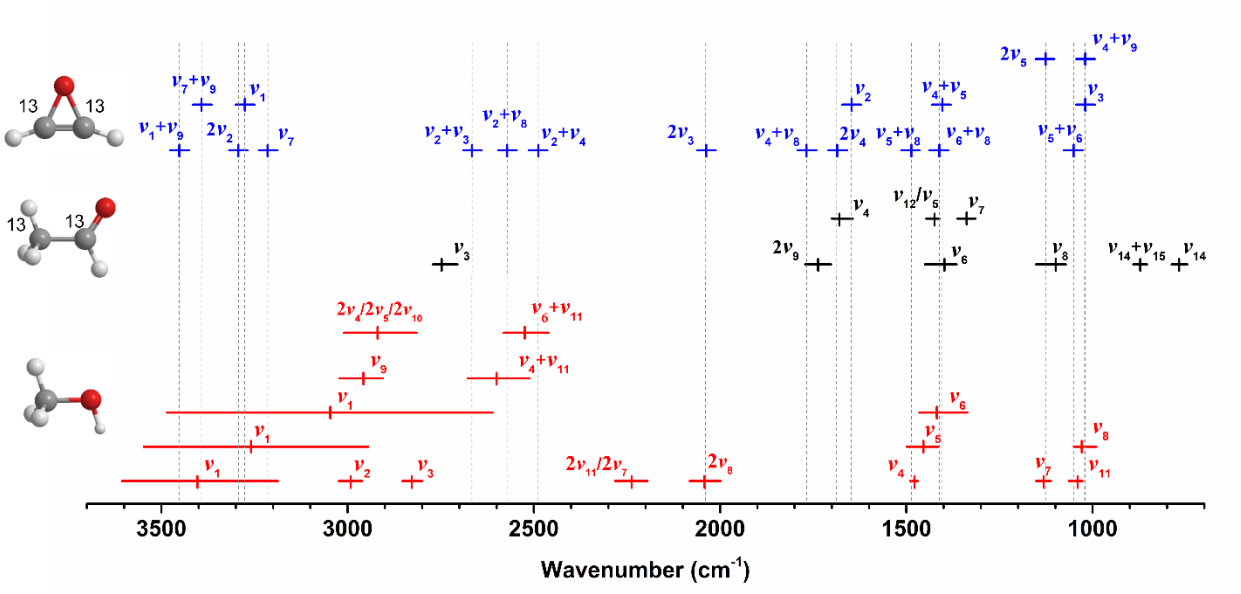

Fig. S8. Peak absorptions (solid vertical lines) and absorption ranges (solid horizontal lines) of methanol (CH_3OH, red), acetaldehyde-$^{13}C_2$ ($^{13}CH_3{}^{13}CHO$, black), and oxirene-$^{13}C_2$ (*c*-$^{13}C_2H_2O$, blue). Dotted vertical lines indicate the overlap positions between the absorption peaks of oxirene-$^{13}C_2$ and reactants (CH_3OH, red; $^{13}CH_3{}^{13}CHO$, black). Detailed absorption positions and assignments for experimentally measured methanol and acetaldehyde-$^{13}C_2$ ices as well as calculated oxirene-$^{13}C_2$ are listed in table S8.

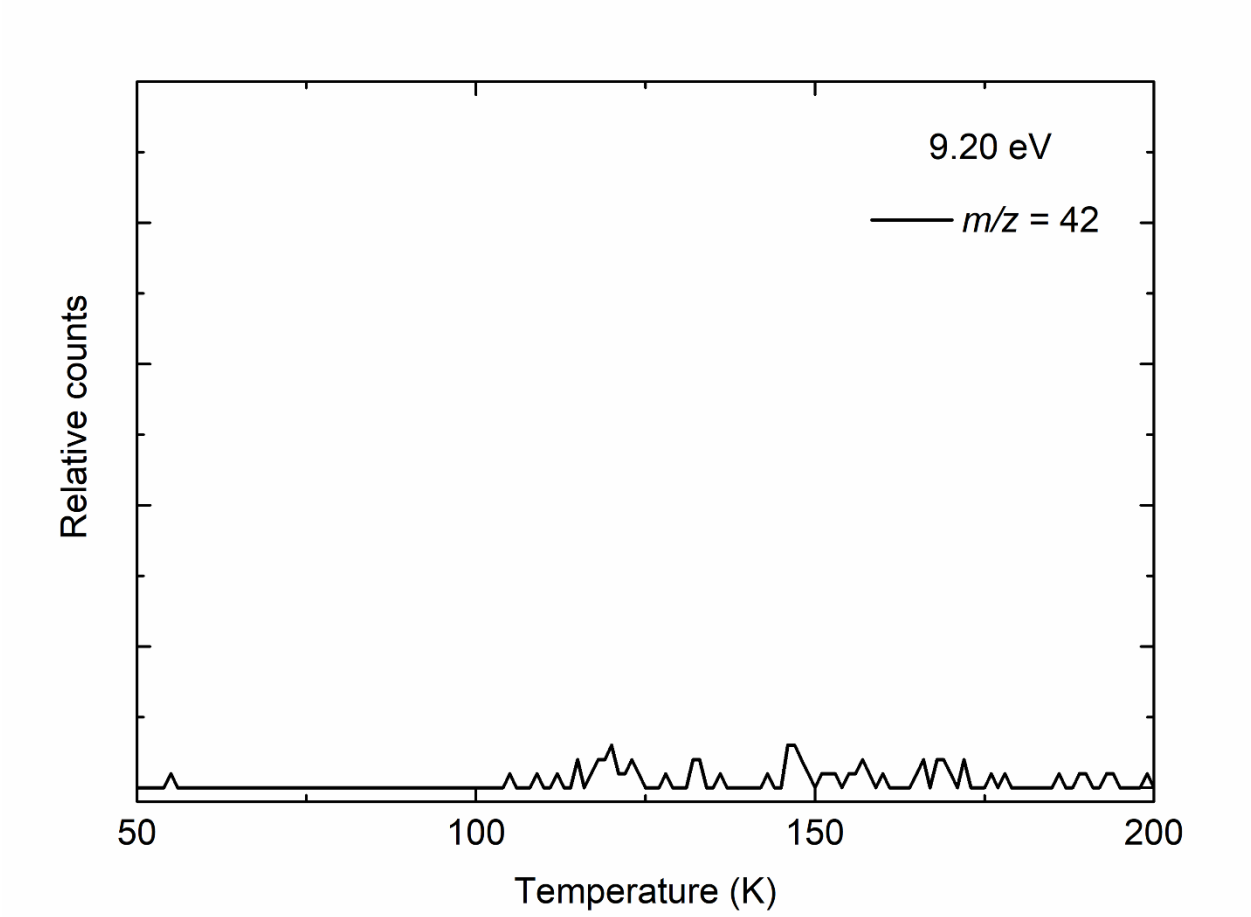

Fig. S9. PI-ReTOF-MS data recorded at 9.20 eV during the temperature-TPD phase of irradiated (20 nA, 15 minutes) CH_3CHO ice. TPD desorption profile of ion signal for *m/z* = 42 shows no evidence for the formation of oxirene.

Table S1.
Absorption peaks observed in CH_3OH−CH_3CHO ice before and after electron irradiation (20 nA, 15 minutes) at 5 K.

Pristine ice, before irradiation (cm^{-1})	
CH_3OH	Assignment[a]
3402, 3261, 3048	ν_1
2991	ν_2
2955	ν_9
2914	$2\nu_4$ / $2\nu_5$ / $2\nu_{10}$
2825	ν_3
2594	$\nu_4 + \nu_{11}$
2517	$\nu_6 + \nu_{11}$
2233	$2\nu_{11}$/$2\nu_7$
2038	$2\nu_8$
1475	ν_4
1455	ν_5
1420	ν_6
1033	ν_8
CH_3CHO	Assignment[b]
2866	$2\nu_6$
2760	ν_3
1767	$2\nu_9$
1718	ν_4
1430	ν_{12} / ν_5
1392	ν_6
1345	ν_7
1122	ν_8
887	$\nu_{14} + \nu_{15}$
777	ν_{14}
New absorption after irradiation (cm^{-1})	Assignment[b]
2130	ν (CO)
1842	$CH_3C\dot{O}$ ν(CO)

[a] Assignments based on references (*29*, *71*).
[b] Assignments based on reference (*30*).

Table S2.
Absorption peaks observed in CH_3OH−CH_3CHO ice before and after electron irradiation (20 nA, 60 minutes) at 5 K.

Pristine ice, before irradiation (cm^{-1})	
CH_3OH	Assignment[a]
3402, 3261, 3048	ν_1
2993	ν_2
2955	ν_9
2920	$2\nu_4$ / $2\nu_5$ / $2\nu_{10}$
2824	ν_3
2598	$\nu_4 + \nu_{11}$
2521	$\nu_6 + \nu_{11}$
2237	$2\nu_{11}$/$2\nu_7$
2038	$2\nu_8$
1475	ν_4
1455	ν_5
1420	ν_6
1029	ν_8
CH_3CHO	Assignment[b]
2866	$2\nu_6$
2760	ν_3
1767	$2\nu_9$
1718	ν_4
1431	ν_{12} / ν_5
1392	ν_6
1345	ν_7
1122	ν_8
887	$\nu_{14} + \nu_{15}$
773	ν_{14}
New absorption after irradiation (cm^{-1})	Assignment[c]
2129	ν (CO)
1840	$CH_3C\dot{O}$ ν(CO)
1306	ν_4 (CH_4)
1199	ν_4 ($\dot{C}H_2OH$)

[a] Assignments based on references (*29*, *71*).
[b] Assignments based on reference (*30*).
[c] Assignments based on references (*29*, *30*).

Table S3.
Absorption peaks observed in CH_3OH–$^{13}CH_3{}^{13}CHO$ ice before and after electron irradiation (20 nA, 15 minutes) at 5 K.

Pristine ice, before irradiation (cm^{-1})	
CH_3OH	Assignment[a]
3402, 3261, 3048	ν_1
2983	ν_2
2954	ν_9
2912	$2\nu_4$ / $2\nu_5$ / $2\nu_{10}$
2826	ν_3
2596	$\nu_4 + \nu_{11}$
2520	$\nu_6 + \nu_{11}$
2229	$2\nu_{11}/2\nu_7$
1476	ν_4
1455	ν_5
1032	ν_8
$^{13}CH_3{}^{13}CHO$	Assignment
2748	ν_3
1738	$2\nu_9$
1678	ν_4
1423	ν_{12} / ν_5
1397	ν_6
1336	ν_7
1102	ν_8
871	$\nu_{14} + \nu_{15}$
768	ν_{14}
New absorption after irradiation (cm^{-1})	Assignment
2087	ν (^{13}CO) [b]
2066	ν ($^{13}CH_2{}^{13}CO$)[b]
1802	$^{13}CH_3{}^{13}C\dot{O}$ ν(^{13}CO)

[a] Assignments based on references (*29*, *71*).
[b] Assignments based on reference (*31*).

Table S4.
Absorption positions of methanol (CH_3OH), acetaldehyde (CH_3CHO), and oxirene (c-C_2H_2O). The numbers in brackets show the widths of the peaks observed in pure methanol or acetaldehyde ice (*54*, *72*).

Absorptions of methanol (cm^{-1})	Assignment[a]
3402 (419), 3261 (602), 3048 (874)	ν_1
2993 (63)	ν_2
2956 (116)	ν_9
2920 (195)	$2\nu_4$ / $2\nu_5$ / $2\nu_{10}$
2828 (53)	ν_3
2600 (166)	$\nu_4 + \nu_{11}$
2525 (120)	$\nu_6 + \nu_{11}$
2237 (87)	$2\nu_{11}$/$2\nu_7$
2042 (83)	$2\nu_8$
1478 (21)	ν_4
1455 (84)	ν_5
1420 (129)	ν_6
1130 (40)	ν_7
1040 (37)	ν_{11}
1030 (61)	ν_8
Absorptions of acetaldehyde (cm^{-1})	**Assignment[b]**
3416 (58)	$2\nu_4$
3001 (51)	ν_1
2916 (35)	ν_2
2865 (97)	$2\nu_6$
2759 (85)	ν_3
1769 (55)	$2\nu_9$
1718 (46)	ν_4
1430 (50)	ν_{12} / ν_5
1392 (27)	ν_6
1347 (39)	ν_7
1123 (45)	ν_8
886 (38)	$\nu_{14} + \nu_{15}$
772 (43)	ν_{14}
Calculated absorptions of oxirene (cm^{-1})[c]	**Assignment[c]**
3419	$\nu_1 + \nu_9$
3402	$2\nu_2$
3338	$\nu_7 + \nu_9$
3282	ν_1
3201	ν_7
2740	$\nu_2 + \nu_3$
2625	$\nu_2 + \nu_8$
2549	$\nu_2 + \nu_4$
2244	$\nu_2 + \nu_5$
1772	$\nu_4 + \nu_8$

1701	ν_2
1696	$2\nu_4$
1467	$\nu_5 + \nu_8$
1401	$\nu_6 + \nu_8$
1391	$\nu_4 + \nu_5$
1325	$\nu_4 + \nu_6$
1061	$\nu_8 + \nu_9$
1039	ν_3
1020	$\nu_5 + \nu_6$
924	ν_8
848	ν_4
543	ν_5
477	ν_6
137	ν_9

[a] Assignments based on references (*29*, *71*).

[b] Assignments based on reference (*30*).

[c] Calculated frequencies obtained from CCCBDB Vibrational Listing Page (nist.gov), computed at the CCSD(T)=FULL/cc-pVTZ level. The frequency error of oxirene is estimated to be 25 cm^{-1}.

Table S5.

Error analysis of adiabatic ionization energies (IEs) and relative energies (ΔE) of distinct C_2H_2O isomers; IEs and ΔE were computed at the CCSD(T)/CBS(aug-T,Q)//CCSD(T)/aug-cc-pVTZ level of theory including the zero-point vibrational energy corrections. An offset of 0.03 eV was subtracted to correct for the electric field effect. The computed Cartesian coordinates and vibrational frequencies are shown in table S11. The combined error limits of −0.05 - +0.03 eV were used based on the calculated ionization energies and experimental ionization energies of different carbon-, hydrogen-, and oxygen- containing compounds (*73*).

Isomer	Structure	ΔE (kJ mol^{-1})	Experimental IE (eV)	Computed IE (eV)	IE range after error analysis (eV)	Corrected IE with electric field effect (eV)
1 Oxirene		314		8.66	8.61 – 8.69	8.58 – 8.66
2 Ketene		0	9.617 ± 0.003 (*25*)	9.61	9.56 – 9.64	9.53 – 9.61
3 Oxiranylidene		256		9.85	9.80 – 9.88	9.77 – 9.85
4 Ethynol	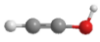	139		10.03	9.98 – 10.06	9.95 – 10.03
5 Formylcarbene (triplet)		311		6.38	6.33 – 6.41	6.30 – 6.38
Acetone			9.703 ± 0.006	9.71		
Propanal			9.96 ± 0.01	9.97		
Propylene oxide			10.22 ± 0.02	10.24		
2-Propen-1-ol			9.67 ± 0.03	9.65		
Methanol			10.84 ± 0.01	10.86		
Propadienone			9.12 ± 0.05	9.15		
Formaldehyde			10.88 ± 0.01	10.89		
Acetaldehyde			10.229 ± 0.0007	10.24		

Table S6.
Absorption positions of methanol (CH_3OH), acetaldehyde-d_3 (CD_3CHO), and oxirene-d_2 (*c*-C_2D_2O). The numbers in brackets show the widths of the peaks observed in pure methanol or acetaldehyde-d_3 ice (*55, 30*).

Absorptions of methanol (cm^{-1})	Assignment[a]
3402 (419), 3261 (602), 3048 (874)	ν_1
2993 (63)	ν_2
2956 (116)	ν_9
2920 (195)	$2\nu_4$ / $2\nu_5$ / $2\nu_{10}$
2828 (53)	ν_3
2600 (166)	$\nu_4 + \nu_{11}$
2525 (120)	$\nu_6 + \nu_{11}$
2237 (87)	$2\nu_{11}/2\nu_7$
2042 (83)	$2\nu_8$
1478 (21)	ν_4
1455 (84)	ν_5
1420 (129)	ν_6
1130 (40)	ν_7
1040 (37)	ν_{11}
1030 (61)	ν_8
Absorptions of acetaldehyde-d_3 (cm^{-1})	**Assignment[b]**
3405 (95)	$2\nu_4$
2853 (112)	$2\nu_5$
2749 (69)	ν_1
2252 (18)	ν_2
2228 (21)	ν_{11}
2118 (22)	ν_3
1890 (73)	$\nu_6 + \nu_9$
1711 (114)	ν_4
1397 (58)	ν_5
1138 (40)	ν_6
1029 (47)	ν_7
963 (36)	ν_8
Calculated absorptions of oxirene-d_2 (cm^{-1})[c]	**Assignment[c]**
3512	$\nu_1 + \nu_3$
3330	$\nu_3 + \nu_7$
3268	$\nu_1 + \nu_8$
3198	$\nu_1 + \nu_4$
3128	$2\nu_2$
3085	$\nu_7 + \nu_8$
3018	$\nu_1 + \nu_5$
3015	$\nu_4 + \nu_7$
2913	$\nu_1 + \nu_6$
2835	$\nu_5 + \nu_7$
2730	$\nu_6 + \nu_7$

2725	$\nu_1 + \nu_9$
2546	ν_1
2543	$\nu_7 + \nu_9$
2216	$\nu_2 + \nu_4$
2036	$\nu_2 + \nu_5$
1931	$\nu_2 + \nu_6$
1743	$\nu_2 + \nu_9$
1688	$\nu_3 + \nu_8$
1444	$2\nu_8$
1438	$\nu_3 + \nu_5$
1146	$\nu_3 + \nu_9$
1124	$\nu_4 + \nu_5$
1019	$\nu_4 + \nu_6$
966	ν_3

[a] Assignments based on references (*29*, *71*).
[b] Assignments based on reference (*30*).
[c] Calculated frequencies at CCSD(T)/aug-cc-pVTZ level of theory with scaled factor of 0.970. The frequency error is estimated to be 25 cm^{-1}.

Table S7.
Absorption positions of methanol-d_3 (CD_3OH), acetaldehyde-d_4 (CD_3CDO), and oxirene-d_2 (*c*-C_2D_2O). The numbers in brackets show the widths of the peaks observed in pure methanol-d_3 or acetaldehyde-d_4 ice (*72*, *74*).

Absorptions of methanol-d_3 (cm^{-1})	Assignment[a]
3460 (193), 3380 (225), 3250 (681)	ν_1
2780 (204)	$2\nu_6$
2509 (69)	$\nu_5 + \nu_6$
2233 (77)	ν_2
2214 (90)	ν_9
2140 (58)	$2\nu_{10}$
2070 (50)	ν_3
2009 (12)	$2\nu_4$
1958 (57)	$2\nu_8$
1414 (339)	ν_6
1123 (48)	ν_5
1067 (45)	ν_4
987 (57)	ν_8
898 (54)	ν_7
880 (28)	ν_{11}
Absorptions of acetaldehyde-d_4 (cm^{-1})	**Assignment[b]**
3384 (74)	$2\nu_4$
2254 (27)	ν_1
2219 (30)	ν_{11}
2134 (36)	ν_2
2104 (37)	ν_3
1908 (49)	$\nu_5 + \nu_9$
1709 (60)	ν_4
1693 (45)	$\nu_8 + \nu_9$
1157 (49)	ν_5
1042 (43)	ν_{12}
1021 (35)	ν_6
952 (40)	ν_{13}
941 (20)	ν_8
Calculated absorptions of oxirene-d_2 (cm^{-1})[c]	**Assignment[c]**
3512	$\nu_1 + \nu_3$
3330	$\nu_3 + \nu_7$
3268	$\nu_1 + \nu_8$
3198	$\nu_1 + \nu_4$
3128	$2\nu_2$
3085	$\nu_7 + \nu_8$
3018	$\nu_1 + \nu_5$
3015	$\nu_4 + \nu_7$
2913	$\nu_1 + \nu_6$
2835	$\nu_5 + \nu_7$

2730	$\nu_6 + \nu_7$
2725	$\nu_1 + \nu_9$
2546	ν_1
2216	$\nu_2 + \nu_4$
1933	$2\nu_3$
1931	$\nu_2 + \nu_6$
1688	$\nu_3 + \nu_8$
1564	ν_2
1444	$2\nu_8$
1438	$\nu_3 + \nu_5$
1374	$\nu_4 + \nu_8$
1333	$\nu_3 + \nu_6$
1304	$2\nu_4$
1146	$\nu_3 + \nu_9$
1124	$\nu_4 + \nu_5$
1089	$\nu_6 + \nu_8$
1019	$\nu_4 + \nu_6$
966	ν_3
944	$2\nu_5$
901	$\nu_8 + \nu_9$

[a] Assignments based on references (*74*).
[b] Assignments based on reference (*72*).
[c] Calculated frequencies at CCSD(T)/aug-cc-pVTZ level of theory with scaled factor of 0.970. The frequency error is estimated to be 25 cm^{-1}.

Table S8.
Absorption positions of methanol (CH_3OH), acetaldehyde-$^{13}C_2$ ($^{13}CH_3{}^{13}CHO$), and oxirene-$^{13}C_2$ (*c*-$^{13}C_2H_2O$). The numbers in brackets show the widths of the peaks observed in pure methanol ice (*55*) or determined in mixed CH_3OH–$^{13}CH_3{}^{13}CHO$ ice in this work (acetaldehyde-$^{13}C_2$).

Absorptions of methanol (cm^{-1})	Assignment[a]
3402 (419), 3261 (602), 3048 (874)	ν_1
2993 (63)	ν_2
2956 (116)	ν_9
2920 (195)	$2\nu_4$ / $2\nu_5$ / $2\nu_{10}$
2828 (53)	ν_3
2600 (166)	$\nu_4 + \nu_{11}$
2525 (120)	$\nu_6 + \nu_{11}$
2237 (87)	$2\nu_{11}/2\nu_7$
2042 (83)	$2\nu_8$
1478 (21)	ν_4
1455 (84)	ν_5
1420 (129)	ν_6
1130 (40)	ν_7
1040 (37)	ν_{11}
1030 (61)	ν_8
Absorptions of acetaldehyde-$^{13}C_2$ (cm^{-1})	**Assignment**
2748 (66)	ν_3
1738 (70)	$2\nu_9$
1678 (56)	ν_4
1423 (36)	ν_{12} / ν_5
1397 (85)	ν_6
1336 (48)	ν_7
1102 (80)	ν_8
871 (37)	$\nu_{14} + \nu_{15}$
768 (42)	ν_{14}
Calculated absorptions of oxirene-$^{13}C_2$ (cm^{-1})[b]	**Assignment[b]**
3451	$\nu_1 + \nu_9$
3390	$\nu_7 + \nu_9$
3293	$2\nu_2$
3275	ν_1
3213	ν_7
2665	$\nu_2 + \nu_3$
2571	$\nu_2 + \nu_8$
2489	$\nu_2 + \nu_4$
2037	$2\nu_3$
1767	$\nu_4 + \nu_8$
1684	$2\nu_4$
1647	ν_2
1489	$\nu_5 + \nu_8$
1413	$\nu_6 + \nu_8$

1406	$\nu_4 + \nu_5$
1128	$2\nu_5$
1052	$\nu_5 + \nu_6$
1019	$\nu_4 + \nu_9$
1019	ν_3

[a] Assignments based on references (*29*, *71*).

[b] Calculated frequencies at CCSD(T)/aug-cc-pVTZ level of theory with scaled factor of 0.970. The frequency error is estimated to be 25 cm^{-1}.

Table S9. Calculated CASPT2(16,14) single-point relative energies of various stationary structures along the oxirene → formylcarbene → ketene isomerization pathway with different basis sets and extrapolated to the CBS limit.[a]

	oxirene	singlet formylcarbene	triplet formylcarbene	ketene	oxiranylidene	TS1	TS2	TS3
CASPT2/cc-pVTZ	0.0	0.6	-14.4	-318.0	-50.9	12.0	34.8	11.5
CASPT2/cc-pVQZ	0.0	19.2	-7.8	-314.6	-44.2	12.6	38.6	17.1
CASPT2/cc-pV5Z	0.0	21.3	0.3	-307.2	-41.1	13.5	44.1	20.5
CASPT2/CBS(T,Q)[b]	0.0	32.1	-3.2	-312.2	-39.6	13.1	41.2	21.0
CASPT2/CBS(Q,5)[c]	0.0	23.3	7.8	-300.3	-38.1	14.2	49.3	23.7
CASPT2/CBS(T,Q,5)[d]	0.0	17.3	9.3	-298.3	-38.6	14.5	50.8	23.7
CASPT2/aug-cc-pVTZ	0.0	19.2	-4.1	-305.4	-44.8	17.6	42.8	27.4
CASPT2/aug-cc-pVQZ	0.0	20.2	-0.9	-306.2	-42.8	17.9	44.9	29.3
CASPT2/aug-cc-pV5Z	0.0			-306.1				
CASPT2/CBS(aug-T,Q)[b]	**0.0**	**20.8**	**1.2**	**-306.8**	**-41.5**	**18.1**	**46.3**	**30.7**
CASPT2/CBS(aug-Q,5)[c]	0.0			-305.9				
CASPT2/CBS(aug-T,Q,5)[d]	0.0			-305.6				

[a]Geometries of all structures were optimized at the CCSD(T)/aug-cc-pVTZ level of theory, harmonic ZPE were computed using the same method and anharmonic corrections were evaluated at the PBE0/aug-cc-pVTZ level. ZPE with anharmonic corrections are included in the calculations of relative energies.
[b]The CBS(T,Q) energy is extrapolated as E(VQZ) + 0.69377*{E(VQZ) – E(VTZ)}.
[c]The CBS(Q,5) energy is extrapolated as E(V5Z) + 0.931445*{E(V5Z) – E(VQZ)}.
[d]The CBS(T,Q,5) energy is extrapolated using the exponential decay function in terms of the basis set cardinal number x = 3, 4, and 5.

Table S10.
Parameters for the generation of vacuum ultraviolet (VUV) light used in this work. The uncertainty for VUV photon energies is less than 0.005 eV.

VUV energy (eV)	9.70 ($2\omega_1 - \omega_2$)	9.20 ($2\omega_1 - \omega_2$)	8.25 ($2\omega_1 - \omega_2$)
VUV wavelength (nm)	127.819	134. 765	150.284
Nonlinear medium	Krypton	Xenon	Xenon
ω_1 wavelength (nm)	202.316	222.566	249.628
Nd:YAG output (nm)	532	355	355
Dye laser output (nm)	606.948	445.132	499.256
Dye	Rhodamine 610/640 (0.17/0.04 g L^{-1} ethanol)	Coumarin 450 (0.2 g L^{-1} ethanol)	Coumarin 503 (0.4 g L^{-1} ethanol)
ω_2 wavelength (nm)	484.982	638.667	736.448
Nd:YAG output (nm)	355	532	532
Dye laser output (nm)	484.982	638.667	736.448
Dye	Coumarin 480 (0.4 g L^{-1} ethanol)	DCM (0.3 g L^{-1} DMSO)	LDS 722 (0.25 g L^{-1} ethanol)

Table S11.
Cartesian coordinates for C_2H_2O structures. CCSD(T)/aug-cc-pVTZ optimized geometry (distances in Angstrom), vibrational frequencies (cm^{-1}) of neutral molecules, electronic energies E and E(CBS) (in hartree), zero-point vibrational energies (kcal/mol) as well as Anh. corr. (kcal/mol).

ethynol

H	-1.539319641	0.829856603	0.000000000
O	-1.175065699	-0.063647434	0.000000000
C	0.142513804	0.011189067	0.000000000
C	1.350437908	0.003324672	0.000000000
H	2.412144728	0.007461759	0.000000000

E = -152.3039861
E(CBS) = -152.3776612
ZPVE = 19.7228
Anh. corr. = 0.238

Frequency	**Intensity**
355.1584	9.2506
378.5624	5.3712
527.2053	52.8696
610.2357	45.2486
1061.9691	78.9352
1270.1902	86.8722
2231.0818	128.804
3474.4798	84.2645
3799.153	114.2566

ethynol radical cation

H	-2.424138646	0.011228422	0.000000000
C	-1.349420840	-0.007434067	0.000000000
C	-0.102007022	0.037916682	0.000000000
O	1.139287507	-0.072916693	0.000000000
H	1.624721991	0.783061062	0.000000000

E = -151.9477262
E(CBS) = -152.0081104
ZPVE = 19.1948

formylcarbene singlet

H	-1.460937182	0.841630612	0.705032184
C	-1.034814858	0.243311122	-0.090299065
C	-0.000958848	-0.619432138	0.038600369

O	0.856471853	0.335413094	-0.006169080
H	0.200887458	-1.686471298	0.008443092

E = -152.2342135
E(CBS) = -152.3072744
ZPVE = 18.5247
Anh. corr. = 0.251

Frequency	**Intensity**
296.6473	36.4084
451.6903	229.0214
690.0529	76.5703
972.971	7.3336
1157.7451	34.0687
1399.239	39.9735
1518.6785	15.1998
3165.2661	6.7598
3228.3475	9.1788

formylcarbene triplet

H	-2.276127960	0.152328439	0.000000000
C	-1.271623243	-0.252112350	0.000000000
C	0.011203868	0.381832802	0.000000000
O	1.090966506	-0.200741892	0.000000000
H	-0.030704594	1.489031800	0.000000000

E = -152.2396046
E(CBS) = -152.3100130
ZPVE = 18.5967
Anh. corr. = 0.240

Frequency	**Intensity**
466.9951	11.4264
468.6682	1.1648
873.7371	11.0643
949.0429	0.2516
1115.5953	48.1644
1387.0736	5.6099
1585.4944	74.991
2910.3849	51.1827
3216.4299	0.0856

formylcarbene radical cation (quartet state)

H	-2.273621608	0.072144698	0.000000000
C	-1.240042633	-0.254296397	0.000000000

C	-0.003032170	0.414026168	0.000000000
O	1.069253697	-0.220096767	0.000000000
H	0.104868198	1.519075716	0.000000000

E = -151.8641170
E(CBS) = -151.9202896
ZPVE = 18.1417

ketene

O	0.000000000	0.000000000	-1.188203868
C	0.000000000	0.000000000	-0.020833195
C	0.000000000	0.000000000	1.298512327
H	0.942940379	0.000000000	1.822275579
H	-0.942940379	0.000000000	1.822275579

E = -152.3691021
E(CBS) = -152.4307654
ZPVE = 19.6581
Anh. corr. = 0.216

Frequency	**Intensity**
434.5529	2.6533
506.8637	60.6434
587.6051	46.3401
989.9896	2.0512
1148.6591	4.4311
1411.5277	13.1207
2181.6866	597.6073
3192.6388	25.5261
3297.527	6.9494

ketene radical cation

O	0.000000000	0.000000000	-1.188535282
C	0.000000000	0.000000000	-0.060392428
C	0.000000000	0.000000000	1.334842625
H	0.959012275	0.000000000	1.844128657
H	-0.959012275	0.000000000	1.844128657

E = -152.0180054
E(CBS) = -152.0772688
ZPVE = 19.5556

oxiranylidene

O	-0.501388802	0.544504297	0.000000000
C	-0.442094417	-0.747807189	0.000000000
C	0.875395211	-0.004714980	0.000000000
H	1.399082891	0.159237102	0.931289547
H	1.399082891	0.159237102	-0.931289547

E = -152.2626507
E(CBS) = -152.3334567
ZPVE = 20.2229
Anh. corr. = 0.251

Frequency	**Intensity**
817.9362	30.7101
838.855	41.6549
885.0955	1.845
1101.4491	13.5458
1116.652	1.7738
1399.8045	32.5565
1519.1688	22.043
3146.0007	2.1293
3260.5395	3.7728

oxiranylidene radical cation

O	-0.742156619	0.387278417	0.000000000
C	-0.234199870	-0.706492660	0.000000000
C	0.989752801	0.117266964	0.000000000
H	1.391162394	0.434709955	0.957824939
H	1.391162394	0.434709955	-0.957824939

E = -151.9113247
E(CBS) = -151.9703272
ZPVE = 19.5899

oxirene

H	0.000000000	1.655416097	0.833013394
C	0.000000000	0.637527386	0.502199978
O	0.000000000	0.000000000	-0.858514308
C	0.000000000	-0.637527386	0.502199978
H	0.000000000	-1.655416097	0.833013394

E = -152.2322559
E(CBS) = -152.3079364
ZPVE = 18.0425
Anh. corr. = 0.245

E(CBS, vertical triplet energy) = -152.2041980

Frequency	**Intensity**
187.6211	0.978
505.2871	77.4479
589.646	0
871.9501	56.0558
959.4067	6.8418
1063.3295	8.6286
1757.1488	3.622
3322.1987	47.295
3395.0532	2.7118

oxirene-d_2

Frequency

184.9691
378.3504
486.5991
671.9708
744.0995
996.3052
1612.3625
2436.3624
2624.6654

ZPVE: 14.4898

oxirene-$^{13}C_2$

Frequency
182.1979
503.0574
581.3629
868.1942
953.3973
1050.0613
1697.5996
3312.6092
3376.0271

ZPVE: 17.9047

oxirene radical cation

H	0.000000000	1.695689729	0.753383961
C	0.000000000	0.654300945	0.460958687
O	0.000000000	0.000000000	-0.786597940
C	0.000000000	-0.654300945	0.460958687
H	0.000000000	-1.695689729	0.753383961

E = -151.9319836
E(CBS) = -151.9917672
ZPVE = 19.2440

TS1

H	-1.543948397	1.082500300	0.283804056
C	-0.884778804	0.307549366	-0.041573996
O	0.816440171	0.337399837	0.000968929
C	-0.079728204	-0.699803198	0.014627189
H	0.070670087	-1.766781391	0.021669290

E = -152.2317062
E(CBS) = -152.3064973
ZPVE = 17.8351
Anh. corr. = 0.244
ν_i = 268.0464

TS2

H	-1.726214663	0.366910914	0.903209042
C	-1.293409365	0.200293197	-0.097767460
C	0.012518619	-0.394621461	0.015949355
O	1.072548598	0.217917731	0.003060475
H	-0.044563270	-1.511590102	0.022413133

E = -152.2255527
E(CBS) = -152.2981266
ZPVE = 17.3561
Anh. corr. = 0.240
ν_i = 402.5632

TS3

O	-0.895020511	0.333300518	0.033919008
C	-0.232179735	-0.654870281	-0.040303235
C	1.194162738	0.111821762	-0.051833091
H	1.122618339	1.149446916	-0.391629519
H	1.627839871	0.026817629	0.950361704

E = -152.2358648
E(CBS)= -152.2952409
Anh. corr. = 0.240
ZPVE = 17.5871

vi = 500.2473

REFERENCES

1. M. Berthelot, Sceances Acad. Sci. 70, 256 (1870). *Bull. Soc. Chim. France [2]* 14, 113 (1870).

2. E. G. Lewars, in *Modeling Marvels: Computational Anticipation of Novel Molecules* (Springer Netherlands, 2008), pp. 31–52.

3. S. J. Klippenstein, L. B. Harding, B. Ruscic, Ab initio computations and active thermochemical tables hand in hand: Heats of formation of core combustion species. *J. Phys. Chem. A* **121**, 6580–6602 (2017).

4. I. G. Csizmadia, J. Font, O. P. Strausz, Mechanism of the Wolff rearrangement. *J. Am. Chem. Soc.* **90**, 7360–7361 (1968).

5. S. A. Matlin, P. G. Sammes, Decomposition of α-diazo-ketones: The oxiren–oxocarbene equilibrium. *J. Chem. Soc. Perkin Trans.* **1**, 2623–2630 (1972).

6. J. F. Liebman, A. Greenberg, A survey of strained organic molecules. *Chem. Rev.* **76**, 311–365 (1976).

7. R. C. Mawhinney, J. D. Goddard, Assessment of density functional theory for the prediction of the nature of the oxirene stationary point. *J. Mol. Struct. Theochem* **629**, 263–270 (2003).

8. E. Lewars, Benzooxirene. Ab initio calculations. *J. Mol. Struct. Theochem* **360**, 67–80 (1996).

9. O. P. Strausz, R. K. Gosavi, A. S. Denes, I. G. Csizmadia, Mechanism of the Wolff rearrangement. 6. Ab initio molecular orbital calculations on the thermodynamic and kinetic stability of the oxirene molecule. *J. Am. Chem. Soc.* **98**, 4784–4786 (1976).

10. C. Bachmann, T. Y. N'Guessan, F. Debu, M. Monnier, J. Pourcin, J. P. Aycard, H. Bodot, Oxirenes and ketocarbenes from α-diazoketone photolysis: Experiments in rare gas matrices. Relative stabilities and isomerization barriers from MNDOC-BWEN calculations. *J. Am. Chem. Soc.* **112**, 7488–7497 (1990).

11. F. Turecek, D. E. Drinkwater, F. W. McLafferty, Gas-phase formation and rearrangements of methyloxirene and its cation radical. *J. Am. Chem. Soc.* **113**, 5958–5964 (1991).

12. W. J. Bouma, R. H. Nobes, L. Radom, C. Woodward, Existence of stable structural isomers of ketene. A theoretical study of the C_2H_2O potential energy surface. *J. Org. Chem.* **47**, 1869–1875 (1982).

13. A. P. Scott, R. H. Nobes, H. F. Schaefer, L. Radom, The Wolff rearrangement: The relevant portion of the oxirene-ketene potential energy hypersurface. *J. Am. Chem. Soc.* **116**, 10159–10164 (1994).

14. W. Kirmse, 100 years of the Wolff rearrangement. *Eur. J. Org. Chem.* **2002**, 2193–2256 (2002).

15. M. Torres, J. L. Bourdelande, A. Clement, O. P. Strausz, Argon-matrix isolation of bis(trifluoromethyl)oxirene, perfluoromethylethyloxirene, and their isomeric ketocarbenes. *J. Am. Chem. Soc.* **105**, 1698–1700 (1983).

16. P. Carsky, B. A. Hess Jr., L. J. Schaad, Ab initio study of the structures and vibrational spectra of the Hueckel 4n heterocycles azirine, oxirene and thiirene. *J. Am. Chem. Soc.* **105**, 396–402 (1983).

17. G. Vacek, J. M. Galbraith, Y. Yamaguchi, H. F. Schaefer, R. H. Nobes, A. P. Scott, L. Radom, Oxirene: To be or not to be? *J. Phys. Chem.* **98**, 8660–8665 (1994).

18. P. J. Wilson, D. J. Tozer, A Kohn-Sham study of the oxirene-ketene potential energy surface. *Chem. Phys. Lett.* **352**, 540–544 (2002).

19. E. G. Lewars, in *Computational Chemistry: Introduction to the Theory and Applications of Molecular and Quantum Mechanics* (Springer International Publishing, 2016), pp. 613–643.

20. A. Rey Planells, A. Espinosa Ferao, Accurate ring strain energies of unsaturated three-membered heterocycles with one group 13–16 element. *Inorg. Chem.* **61**, 6459–6468 (2022).

21. A. Karton, D. Talbi, Pinning the most stable $H_xC_yO_z$ isomers in space by means of high-level theoretical procedures. *Chem. Phys.* **436-437**, 22–28 (2014).

22. M. Torres, A. Clement, O. P. Strausz, Photolysis of vinylene thioxocarbonates: A new source of ketocarbenes. *J. Org. Chem.* **45**, 2271–2273 (1980).

23. C. E. C. A. Hop, J. L. Holmes, J. K. Terlouw, The oxirene radical cation and its neutralization in the gas phase. *J. Am. Chem. Soc.* **111**, 441–445 (1989).

24. R. Hochstrasser, J. Wirz, Reversible photoisomerization of ketene to ethynol. *Angew. Chem. Int. Ed.* **29**, 411–413 (1990).

25. J. P. Toscano, M. S. Platz, V. Nikolaev, Lifetimes of simple ketocarbenes. *J. Am. Chem. Soc.* **117**, 4712–4713 (1995).

26. J. P. Toscano, M. S. Platz, V. Nikolaev, Y. Cao, M. B. Zimmt, The lifetime of formylcarbene determined by transient absorption and transient grating spectroscopy. *J. Am. Chem. Soc.* **118**, 3527–3528 (1996).

27. A. M. Turner, R. I. Kaiser, Exploiting photoionization reflectron time-of-flight mass spectrometry to explore molecular mass growth processes to complex organic molecules in interstellar and solar system ice analogs. *Acc. Chem. Res.* **53**, 2791–2805 (2020).

28. A. M. Turner, A. S. Koutsogiannis, N. F. Kleimeier, A. Bergantini, C. Zhu, R. C. Fortenberry, R. I. Kaiser, An experimental and theoretical investigation into the formation of ketene (H_2CCO) and ethynol (HCCOH) in interstellar analog ices. *Astrophys. J.* **896**, 88 (2020).

29. S. Maity, R. I. Kaiser, B. M. Jones, Formation of complex organic molecules in methanol and methanol–carbon monoxide ices exposed to ionizing radiation—A combined FTIR and reflectron time-of-flight mass spectrometry study. *Phys. Chem. Chem. Phys.* **17**, 3081–3114 (2015).

30. N. F. Kleimeier, A. M. Turner, R. C. Fortenberry, R. I. Kaiser, On the formation of the popcorn flavorant 2,3-butanedione ($CH_3COCOCH_3$) in acetaldehyde-containing interstellar ices. *ChemPhysChem* **21**, 1531–1540 (2020).

31. R. L. Hudson, M. J. Loeffler, Ketene formation in interstellar ices: A laboratory study. *Astrophys. J.* **773**, 109 (2013).

32. G. Maier, H. P. Reisenauer, M. Cibulka, Oxiranylidene. *Angew. Chem. Int. Ed.* **38**, 105–108 (1999).

33. S. G. Lias, Ionization energy evaluation, in NIST Chemistry WebBook. *NIST Chemistry WebBook, NIST Standard Reference Database Number 69, National Institute of Standards and Technology*.

34. M. J. Abplanalp, R. I. Kaiser, On the formation of complex organic molecules in the interstellar medium: Untangling the chemical complexity of carbon monoxide-hydrocarbon containing ice analogues exposed to ionizing radiation via a combined infrared and reflectron time-of-flight analysis. *Phys. Chem. Chem. Phys.* **21**, 16949–16980 (2019).

35. S. Maity, R. I. Kaiser, B. M. Jones, Infrared and reflectron time-of-flight mass spectroscopic study on the synthesis of glycolaldehyde in methanol (CH_3OH) and methanol–carbon monoxide (CH_3OH–CO) ices exposed to ionization radiation. *Faraday Discuss.* **168**, 485–516 (2014).

36. S. Kobatake, S. Takami, H. Muto, T. Ishikawa, M. Irie, Rapid and reversible shape changes of molecular crystals on photoirradiation. *Nature* **446**, 778–781 (2007).

37. M. Irie, T. Fukaminato, T. Sasaki, N. Tamai, T. Kawai, A digital fluorescent molecular photoswitch. *Nature* **420**, 759–760 (2002).

38. D. Mei, A. M. Karim, Y. Wang, On the reaction mechanism of acetaldehyde decomposition on Mo (110). *ACS Catal.* **2**, 468–478 (2012).

39. N. F. Kleimeier, A. K. Eckhardt, R. I. Kaiser, A mechanistic study on the formation of acetic acid (CH_3COOH) in polar interstellar analog ices exploiting photoionization reflectron time-of-flight mass spectrometry. *Astrophys. J.* **901**, 84 (2020).

40. C.-S. Lam, J. D. Adams, L. J. Butler, The onset of H^+ ketene products from vinoxy radicals prepared by photodissociation of chloroacetaldehyde at 157 nm. *J. Phys. Chem. A* **120**, 2521–2536 (2016).

41. V. Saheb, S. R. Hashemi, S. M. A. Hosseini, Theoretical studies on the kinetics of multi-channel gas-phase unimolecular decomposition of acetaldehyde. *J. Phys. Chem. A* **121**, 6887–6895 (2017).

42. J. Guan, K. R. Randall, H. F. Schaefer III, H. Li, Formylmethylene: The triplet ground state and the lowest singlet state. *J. Phys. Chem. A* **117**, 2152–2159 (2013).

43. T. J. Lee, P. R. Taylor, A diagnostic for determining the quality of single-reference electron correlation methods. *Int. J. Quantum Chem.* **36**, 199–207 (1989).

44. P. Celani, H.-J. Werner, Multireference perturbation theory for large restricted and selected active space reference wave functions. *J. Chem. Phys.* **112**, 5546–5557 (2000).

45. T. Shiozaki, W. Győrffy, P. Celani, H.-J. Werner, Communication: Extended multi-state complete active space second-order perturbation theory: Energy and nuclear gradients. *J. Chem. Phys.* **135**, 081106 (2011).

46. D. J. Goebbert, D. Khuseynov, A. Sanov, O^- + acetaldehyde reaction products: Search for singlet formylmethylene, a Wolff rearrangement intermediate. *J. Phys. Chem. A* **115**, 3208–3217 (2011).

47. J. Cao, Generalized resonance energy transfer theory: Applications to vibrational energy flow in optical cavities. *J. Phys. Chem. Lett.* **13**, 10943–10951 (2022).

48. M. J. Barlow, B. M. Swinyard, P. J. Owen, J. Cernicharo, H. L. Gomez, R. J. Ivison, O. Krause, T. L. Lim, M. Matsuura, S. Miller, G. Olofsson, E. T. Polehampton, Detection of a noble gas molecular ion, $^{36}ArH^+$, in the Crab Nebula. *Science* **342**, 1343–1345 (2013).

49. J. Cernicharo, C. Kahane, J. Gomez-Gonzalez, M. Guelin, Tentative detection of the C_5H radical. *Astron. Astrophys.* **164**, L1–L4 (1986).

50. L. N. Zack, D. T. Halfen, L. M. Ziurys, Detection of FeCN ($X^4\Delta_i$) in IRC+10216: A new interstellar molecule. *Astrophys. J.* **733**, L36 (2011).

51. A. M. Turner, M. J. Abplanalp, S. Y. Chen, Y. T. Chen, A. H. Chang, R. I. Kaiser, A photoionization mass spectroscopic study on the formation of phosphanes in low temperature phosphine ices. *Phys. Chem. Chem. Phys.* **17**, 27281–27291 (2015).

52. M. Bouilloud, N. Fray, Y. Benilan, H. Cottin, M. C. Gazeau, A. Jolly, Bibliographic review and new measurements of the infrared band strengths of pure molecules at 25 K: H_2O, CO_2, CO, CH_4, NH_3, CH_3OH, HCOOH and H_2CO. *Mon. Not. R. Astron. Soc.* **451**, 2145–2160 (2015).

53. R. L. Hudson, F. M. Coleman, Infrared intensities and molar refraction of amorphous dimethyl carbonate—Comparisons to four interstellar molecules. *Phys. Chem. Chem. Phys.* **21**, 11284–11289 (2019).

54. D. M. Hudgins, S. A. Sandford, L. J. Allamandola, A. G. Tielens, Mid- and far-infrared spectroscopy of ices: Optical constants and integrated absorbances. *Astrophys. J. Suppl. Ser.* **86**, 713–870 (1993).

55. C. Zhu, A. M. Turner, C. Meinert, R. I. Kaiser, On the production of polyols and hydroxycarboxylic acids in interstellar analogous ices of methanol. *Astrophys. J.* **889**, 134 (2020).

56. D. Drouin, A. R. Couture, D. Joly, X. Tastet, V. Aimez, R. Gauvin, CASINO V2.42—A fast and easy-to-use modeling tool for scanning electron microscopy and microanalysis users. *Scanning* **29**, 92–101 (2007).

57. M. J. Frisch, G. W. Trucks, H. B. Schlegel, G. E. Scuseria, M. A. Robb, J. R. Cheeseman, G. Scalmani, V. Barone, G. A. Petersson, H. Nakatsuji, X. Li, M. Caricato, A. V. Marenich, J. Bloino, B. G. Janesko, R. Gomperts, B. Mennucci, H. P. Hratchian, J. V. Ortiz, A. F. Izmaylov, J. L. Sonnenberg, Williams, F. Ding, F. Lipparini, F. Egidi, J. Goings, B. Peng, A. Petrone, T. Henderson, D. Ranasinghe, V. G. Zakrzewski, J. Gao, N. Rega, G. Zheng, W. Liang, M. Hada, M. Ehara, K. Toyota, R. Fukuda, J. Hasegawa, M. Ishida, T. Nakajima, Y. Honda, O. Kitao, H. Nakai, T. Vreven, K. Throssell, J. A. Montgomery Jr., J. E. Peralta, F. Ogliaro, M. J. Bearpark, J. J. Heyd, E. N. Brothers, K. N. Kudin, V. N. Staroverov, T. A. Keith, R. Kobayashi, J. Normand, K. Raghavachari, A. P. Rendell, J. C. Burant, S. S. Iyengar, J. Tomasi, M. Cossi, J. M. Millam, M. Klene, C. Adamo, R. Cammi, J. W. Ochterski, R. L. Martin, K. Morokuma, O. Farkas, J. B. Foresman, D. J. Fox, *Gaussian 16* (Gaussian Inc., 2016).

58. A. D. Becke, Density-functional exchange-energy: Approximation with correct asymptotic behavior. *Phys. Rev. A* **38**, 3098–3100 (1988).

59. C. Lee, W. Yang, R. G. Parr, Development of the Colle-Salvetti correlation-energy formula into a functional of the electron density. *Phys. Rev. B* **37**, 785–789 (1988).

60. A. D. Becke, Density-functional thermochemistry. III. The role of exact exchange. *J. Chem. Phys.* **98**, 5648–5652 (1993).

61. T. H. Dunning, Gaussian basis sets for use in correlated molecular calculations. I. The atoms boron through neon and hydrogen. *J. Chem. Phys.* **90**, 1007–1023 (1989).

62. D. A. Matthews, L. Cheng, M. E. Harding, F. Lipparini, S. Stopkowicz, T.-C. Jagau, P. G. Szalay, J. Gauss, J. F. Stanton, Coupled-cluster techniques for computational chemistry: The CFOUR program package. *J. Chem. Phys.* **152**, 214108 (2020).

63. J. Čížek, On the correlation problem in atomic and molecular systems. Calculation of wavefunction components in Ursell-type expansion using quantum-field theoretical methods. *J. Chem. Phys.* **45**, 4256–4266 (1966).

64. K. Raghavachari, Electron correlation techniques in quantum chemistry: Recent advances. *Annu. Rev. Phys. Chem.* **42**, 615–642 (1991).

65. R. J. Bartlett, J. D. Watts, S. A. Kucharski, J. Noga, Non-iterative fifth-order triple and quadruple excitation energy corrections in correlated methods. *Chem. Phys. Lett.* **165**, 513–522 (1990).

66. R. A. Kendall, T. H. Dunning Jr, R. J. Harrison, Electron affinities of the first-row atoms revisited. Systematic basis sets and wave functions. *J. Chem. Phys.* **96**, 6796–6806 (1992).

67. J. F. Stanton, Why CCSD(T) works: A different perspective. *Chem. Phys. Lett.* **281**, 130–134 (1997).

68. F. Neese, Software update: The ORCA program system, version 4.0. *WIREs Comput. Mol. Sci.* **8**, e1327 (2018).

69. K. A. Peterson, D. E. Woon, T. H. Dunning Jr., Benchmark calculations with correlated molecular wave functions. IV. The classical barrier height of the $H+H_2 \rightarrow H_2+H$ reaction. *J. Chem. Phys.* **100**, 7410–7415 (1994).

70. H.-J. Werner, P. J. Knowles, G. Knizia, F. R. Manby, M. Schütz, P. Celani, W. Györffy, D. Kats, T. Korona, R. Lindh, A. Mitrushenkov, G. Rauhut, K. R. Shamasundar, T. B. Adler, R. D. Amos, S. J. Bennie, A. Bernhardsson, A. Berning, D. L. Cooper, M. J. O. Deegan, A. J. Dobbyn, F. Eckert, E. Goll, C. Hampel, A. Hesselmann, G. Hetzer, T. Hrenar, G. Jansen, C. Köppl, S. J. R. Lee, Y. Liu, A. W. Lloyd, Q. Ma, R. A. Mata, A. J. May, S. J. McNicholas, W. Meyer, T. F. Miller III, M. E. Mura, A. Nicklass, D. P. O'Neill, P. Palmieri, D. Peng, T. Petrenko, K. Pflüger, R. Pitzer, M. Reiher, T. Shiozaki, H. Stoll, A. J. Stone, R. Tarroni, T. Thorsteinsson, M. Wang, and M. Welborn, MOLPRO, version 2021.2. A package of ab initio programs (University of Cardiff, 2021); www.molpro.net.

71. N. F. Kleimeier, A. K. Eckhardt, R. I. Kaiser, Identification of glycolaldehyde enol (HOHC═CHOH) in interstellar analogue ices. *J. Am. Chem. Soc.* **143**, 14009–14018 (2021).

72. N. F. Kleimeier, R. I. Kaiser, Interstellar enolization-acetaldehyde (CH_3CHO) and vinyl alcohol ($H_2CCH(OH)$) as a case study. *ChemPhysChem* **22**, 1229–1236 (2021).

73. C. Zhu, N. F. Kleimeier, A. M. Turner, S. K. Singh, R. C. Fortenberry, R. I. Kaiser, Synthesis of methanediol [$CH_2(OH)_2$]: The simplest geminal diol. *Proc. Natl. Acad. Sci. U.S.A.* **119**, e2111938119 (2022).

74. C. Zhu, R. Frigge, A. Bergantini, R. C. Fortenberry, R. I. Kaiser, Untangling the formation of methoxymethanol (CH_3OCH_2OH) and dimethyl peroxide (CH_3OOCH_3) in star-forming regions. *Astrophys. J.* **881**, 156 (2019).